Ca^{2+} allostery in PTH-receptor signaling

Alex D. White[a,b], Fei Fang[a], Frédéric G. Jean-Alphonse[a], Lisa J. Clark[a,c], Hyun-Jung An[a,d], Hongda Liu[a], Yang Zhao[a], Shelley L. Reynolds[a], Sihoon Lee[d], Kunhong Xiao[a,e,1], Ieva Sutkeviciute[a,1], and Jean-Pierre Vilardaga[a,1]

[a]Department of Pharmacology and Chemical Biology, School of Medicine, University of Pittsburgh, Pittsburgh, PA 15261; [b]Graduate Program in Molecular Pharmacology, School of Medicine, University of Pittsburgh, Pittsburgh, PA 15261; [c]Graduate Program in Molecular Biophysics and Structural Biology, School of Medicine, University of Pittsburgh, Pittsburgh, PA 15261; [d]Department of Internal Medicine and Laboratory of Molecular Endocrinology, Gachon University School of Medicine, Incheon 21565, South Korea; and [e]Vascular Medicine Institute, University of Pittsburgh, School of Medicine, Pittsburgh, PA 15261

Edited by Robert J. Lefkowitz, Howard Hughes Medical Institute and Duke University Medical Center, Durham, NC, and approved December 28, 2018 (received for review August 25, 2018)

The parathyroid hormone (PTH) and its related peptide (PTHrP) activate PTH receptor (PTHR) signaling, but only the PTH sustains G_s-mediated adenosine 3′,5′-cyclic monophosphate (cAMP) production after PTHR internalization into early endosomes. The mechanism of this unexpected behavior for a G-protein–coupled receptor is not fully understood. Here, we show that extracellular Ca^{2+} acts as a positive allosteric modulator of PTHR signaling that regulates sustained cAMP production. Equilibrium and kinetic studies of ligand-binding and receptor activation reveal that Ca^{2+} prolongs the residence time of ligands on the receptor, thus, increasing both the duration of the receptor activation and the cAMP signaling. We further find that Ca^{2+} allostery in the PTHR is strongly affected by the point mutation recently identified in the PTH (PTH^{R25C}) as a new cause of hypocalcemia in humans. Using high-resolution and mass accuracy mass spectrometry approaches, we identified acidic clusters in the receptor's first extracellular loop as key determinants for Ca^{2+} allosterism and endosomal cAMP signaling. These findings coupled to defective Ca^{2+} allostery and cAMP signaling in the PTHR by hypocalcemia-causing PTH^{R25C} suggest that Ca^{2+} allostery in PTHR signaling may be involved in primary signaling processes regulating calcium homeostasis.

PTH | PTH receptor | GPCR signaling | Ca^{2+} allosterism | endosomal cAMP signaling

Recent studies revealed altered modes of adenosine 3′,5′-cyclic monophosphate (cAMP) signaling for G-protein–coupled receptors (GPCRs) where transient cAMP responses originate from cell membrane receptors, whereas internalized receptors prolong cAMP production from intracellular membranes (1–4). Initially uncovered for the parathyroid hormone (PTH) receptor (PTHR), a class B GPCR that primarily couples to Gs/cAMP and Gq/Ca^{2+} signaling pathways and plays a central role in regulating Ca^{2+} homeostasis and bone turnover, this model is considered a new paradigm for GPCR signaling that can be viewed as a new form of signaling bias as it relates to distinct location and duration of cAMP generation (2, 5, 6). Parts of cellular mechanisms of this unexpected process have been determined for the PTHR (7–10), but its structural determinants and relevance for human disease remain unknown. Given that large fluctuations in extracellular Ca^{2+} observed in bone can reach up to 40 mM due to dynamic bone remodeling processes (11) and the reported Ca^{2+} effect on PTH binding on a purified receptor (12), we questioned whether changes in local extracellular Ca^{2+} concentrations could affect PTHR signaling in live cells. Here, we show, through a series of biochemical and cell biological approaches, that extracellular Ca^{2+} binds to the first extracellular loop of the receptor and acts as a positive allosteric modulator of PTHR signaling by increasing ligand residence time on the receptor and amplifying sustained cAMP production. We also show that the sensitivity to Ca^{2+} is lost for the recently identified homozygous PTH variant (R25C), implicated as a novel cause of chronic hypocalcemia in humans (13).

Results

Extracellular Ca^{2+} Prolongs Ligand Residence Time and Promotes Receptor Activation and Endosomal cAMP Production. Both in human embryonic kidney 293 (HEK293) cells and primary osteoblasts expressing recombinant and native PTHR, respectively, we did observe a significant ($P < 0.01$) difference in the duration and magnitude of cAMP production when a range of Ca^{2+} concentrations (0.1–10 mM) was coapplied with the PTH (Fig. 1*A* and *SI Appendix*, Fig. S1, respectively). The effective concentration that gives half of maximal response $(EC)_{50}$ value for the PTH decreased 30-fold when the Ca^{2+} concentration was increased from 0.1 to 10 mM (Fig. 1*B*, *Left*). Ca^{2+} had no effect by itself but caused a concentration-dependent increase in the PTH-mediated cAMP response with an EC_{50} value (1.01 mM) near the physiological range of ionized serum calcium levels (1.1–1.3 mM) (Fig. 1*B*, *Right*). These data show that Ca^{2+} significantly enhances both the magnitude and the duration of PTH-induced cAMP generation. To differentiate the role of Ca^{2+} on cell-surface versus endosomal signaling, we blocked receptor internalization by coexpressing the dominant-negative dynamin mutant K44A (DynK44A). A similar positive effect of Ca^{2+} was maintained for transient cAMP responses originating from the plasma membrane (*SI Appendix*, Fig. S2). To determine

Significance

Blood Ca^{2+} homeostasis is maintained by the actions of the parathyroid hormone (PTH) on its cognate receptor PTHR. PTH binding to PTHR mediates prolonged adenosine 3′,5′-cyclic monophosphate (cAMP) responses in cells after receptor internalization. Here, we show that extracellular Ca^{2+} prolongs the residence time of ligands on the receptor, consequently, increasing both the duration of receptor activation and cAMP signaling. This positive Ca^{2+} allostery is lost for the PTH mutant R25C, recently identified as a new cause of hypocalcemia in humans. Using mass spectrometry approaches, we identify acidic clusters within the first extracellular loop of PTHR as determinants of Ca^{2+} allostery and endosomal cAMP signaling. These findings provide insight into the molecular etiology of hypocalcemia and disease relevance of endosomal cAMP signaling.

Author contributions: I.S. and J.-P.V. designed research; A.D.W., F.F., F.G.J.-A., L.J.C., H.-J.A., H.L., Y.Z., S.L.R., K.X., and I.S. performed research; S.L. contributed new reagents/analytic tools; A.D.W., F.F., F.G.J.-A., L.J.C., H.-J.A., H.L., Y.Z., S.L.R., S.L., K.X., I.S., and J.-P.V. analyzed data; and A.D.W., I.S., and J.-P.V. wrote the paper.

The authors declare no conflict of interest.

This article is a PNAS Direct Submission.

[1]To whom correspondence may be addressed. Email: khxiao@pitt.edu, ies4@pitt.edu, or jpv@pitt.edu.

This article contains supporting information online at www.pnas.org/lookup/suppl/doi:10.1073/pnas.1814670116/-/DCSupplemental.

Published online February 4, 2019.

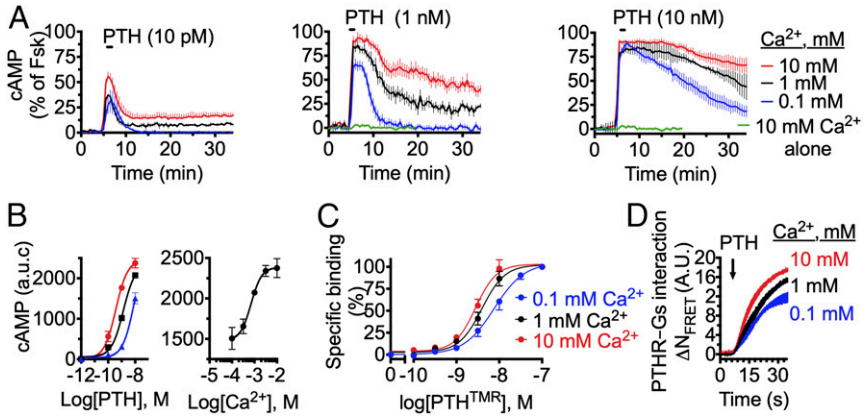

Fig. 1. Allosteric action of extracellular Ca^{2+} on the PTH signaling. (*A*) Averaged cAMP responses over 35 min in HEK293 cells stably expressing the PTHR stimulated with 10 pM, 1 nM, and 10 nM PTH in the presence of a range of [Ca^{2+}]. (*B*) cAMP responses for experiments represented in *A*, determined by measuring the area under the curve (a.u.c) from 0 to 35 min (*Left*). The effect of increasing concentration of Ca^{2+} on the PTH (10 nM)-mediated cAMP (*Right*). (*C*) Saturation-binding isotherms of the PTH^{TMR} (where TMR represents tetramethylrhodamine) to the PTHR stably expressed in HEK293 cells with a range of [Ca^{2+}]. (*D*) Averaged time courses of venus-tagged mini Gs (mGs^{venus}) recruitment to the $PTHR^{CFP}$ (where CFP stands for cyan fluorescent protein) in response to the PTH and in the presence of a range of extracellular [Ca^{2+}] and measured by fluorescence resonance energy transfer (FRET) in HEK293 cells. Data represent the mean ± SEM of $n = 3$ carried out in triplicate for *C* and $n = 8$–12 cells/experiments for *A*, *B*, and *D*.

whether modulation of the PTHR cAMP production was specific to Ca^{2+}, additional experiments were performed using Sr^{2+}, a divalent cation with a hydrodynamic shell similar in size to that of Ca^{2+}. The presence of extracellular Sr^{2+} failed to recapitulate the altered PTH-induced cAMP responses (*SI Appendix*, Fig. S3*A*). Notably, Ca^{2+}-mediated alterations in cAMP production were not extended to the vasopressin type 2 receptor, a class A GPCR with similar endosomal signaling properties as the PTHR (14), suggesting this effect might occur at the level of the ligand–receptor complex (*SI Appendix*, Fig. S3*B*). Surprisingly, potentiation of the PTHR signaling was ligand dependent as the PTHrP-induced cAMP lacked sensitivity to Ca^{2+} (*SI Appendix*, Fig. S3*C*), whereas its analog abaloparatide (ABL), recently Food and Drug Administration approved to treat osteoporosis, showed sensitivity similar to that of the PTH (Fig. 2*A*). We thus utilized either PTH or ABL as a ligand in subsequent experiments.

To further interrogate the mechanism by which extracellular Ca^{2+} regulates receptor signaling, effects on ligand binding were assessed via equilibrium and kinetic analyses. Saturation-binding experiments using tetramethylrhodamine (TMR)-labeled PTH (PTH^{TMR}) revealed moderate increases in ligand-binding affinity in the presence of increasing extracellular Ca^{2+}, a defining characteristic of a positive allosteric modulator (Fig. 1*C*). In an effort to confirm that Ca^{2+}-mediated effects on ligand binding and receptor activation are responsible for the observed modulation of the cAMP response, Gs recruitment to the receptor was measured by FRET using mGs^{venus} and CFP-tagged PTHR ($PTHR^{CFP}$). Even at the saturating concentration of the ligand, increasing extracellular [Ca^{2+}] resulted in enhanced recruitment of the G protein with faster kinetics (Fig. 1*D*).

Consistent with a positive allosteric action, increasing [Ca^{2+}] prolonged ligand residence time ($1/k_{off}$, where k_{off} is the dissociation rate constant) following washout as measured by changes in FRET between TMR-labeled ABL (ABL^{TMR}) and green fluorescent protein (GFP) fused N terminally to PTHR ($PTHR^{GFP}$) (Fig. 2 *B* and *C*). We reasoned that slower ligand dissociation kinetics should, in turn, impact the duration of receptor activation. Accordingly, we utilized a previously characterized FRET-based conformational biosensor ($PTHR^{CFP/YFP}$) to measure the time courses of receptor activation and deactivation by monitoring changes in the FRET ratio upon stimulation and washout, respectively. We observed that increasing [Ca^{2+}] resulted in an increased magnitude of PTHR activation by the PTH and ABL, suggesting a key role in stabilizing the agonist-bound PTHR in an active conformation (Fig. 2 *D* and *E*, *Left*). Ca^{2+} also caused a concentration-dependent increase in deactivation time constants (τ_{off}) after ABL washout (Fig. 2*E*, *Right*), reflective of prolonged receptor activation. Collectively, these results demonstrate that extracellular Ca^{2+} acts as a positive allosteric modulator of the PTHR by prolonging ligand residence time and receptor activation, which, in turn, significantly alters the magnitude and kinetics of the cAMP response.

Mass Spectrometry Evidence of Ca^{2+} Binding to Extracellular Loop 1 of the Receptor. We next sought to identify Ca^{2+}-binding sites on the PTHR through liquid chromatography coupled to tandem mass spectrometry (LC-MS/MS). To this end, two populations of HEK-293S stably expressing the hemagglutinin (HA)-tagged PTHR ($PTHR^{HA}$) were cultured side by side in stable isotope labeling with amino acids in cell culture (SILAC) media containing either "light" (Arg-[$^{12}C_6$,$^{14}N_4$] and Lys-[$^{12}C_6$, $^{14}N_2$]) or "heavy" (Arg-[$^{13}C_6$,$^{15}N_4$] and Lys-[$^{13}C_6$, $^{15}N_2$]) isotopic forms of amino acids. The heavy cells were stimulated with 100 nM PTH(1–34) for 15 min, and the light cells served as a control without any treatment. The PTH stimulation induced receptor C-terminal tail phosphorylation as identified by LC-MS/MS analysis (*SI Appendix*, Fig. S4), indicative of receptor activation upon PTH treatment (15). Mixing lysates from equal numbers of light and heavy cells, the $PTHR^{HA}$ was immunoprecipitated and enzymatically digested by trypsin and subjected to LC-MS/MS analysis using a high-resolution and mass accuracy linear trap quadrupole Orbitrap Velos mass spectrometer. We identified MS peaks (charge state $z = 2$) corresponding to light and heavy versions of the free peptides ^{241}DAVLYSGATLDEAER^{255} (monoisotopic m/z = 805.39252 for light and m/z = 810.39624 for heavy) and ^{256}LTEEELR^{262} (monoisotopic m/z = 445.23596 for light and m/z = 450.23998 for heavy) covering parts of the PTHR's extracellular loop 1 (ECL1) (Fig. 3*A* and *SI Appendix*, Fig. S5). Additional peaks matching exactly the theoretical mass-to-charge change ($\Delta m/z$) when a single Ca^{2+} ion binds to these peptides ($\Delta m/z$ = 18.97347) were simultaneously detected for their corresponding light and heavy versions with monoisotopic m/z = 824.36597 (light) and 829.36926 (heavy) for ^{241}DAVLYSGATLDEAER^{255} and monoisotopic m/z = 464.20917 (light) and = 469.21348 (heavy) for ^{256}LTEEELR^{262} (Fig. 3*A* and *SI Appendix*, Fig. S5). Furthermore, the extent of Ca^{2+} binding was not significantly altered by PTH stimulation.

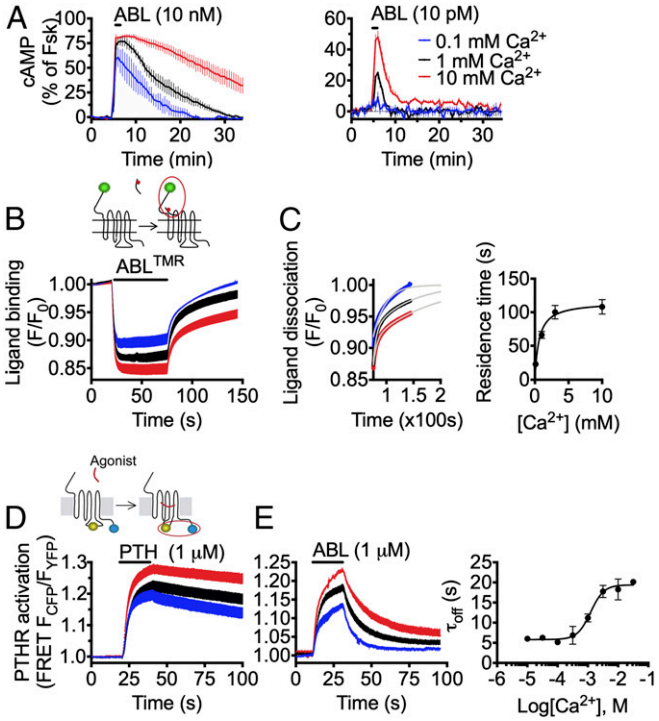

Fig. 2. Ligand residence time determined by Ca^{2+} allostery. (*A*) Averaged cAMP response over 35 min in HEK293 cells stably expressing the PTHR stimulated with 10 nM and 10 pM ABL in the presence of a range of $[Ca^{2+}]$. (*B*) Time courses of ABL-TMR (ABL^{TMR}) binding to the PTHR-GFP expressed in HEK293 cells. Measurements were recorded in single cells continuously perfused with a buffer or 1 μM ABL^{TMR} (horizontal bar) in the presence of varying $[Ca^{2+}]$. (*C*) Comparison of ligand dissociation time courses from experiments in *D* (*Left*) and the corresponding residence time of the ligand, calculated as the inverse of the rate constant of ligand dissociation ($1/\tau_{off}$) as a function of $[Ca^{2+}]$ (*Right*). (*D* and *E*) Effects of Ca^{2+} on time courses of receptor activation/deactivation using the $PTHR^{CFP/YFP}$ (where YFP represents yellow fluorescent protein) stably expressed in HEK293 cells. Single cells were continuously perfused with a buffer or pulsed with 1 μM PTH (*D*) of ABL (*E*, *Left*) for the time indicated by the horizontal bar. Rate constants (τ_{off}) of receptor deactivation (*E*, *Right*) as a function of $[Ca^{2+}]$ calculated from experiments similar to *E* (*Left*). Data represent the mean ± SEM of $n > 3$ and $n = 8$–30 cells/experiment.

These results were confirmed by similar LC-MS/MS analysis performed on a purified receptor (*SI Appendix*, Fig. S6). The same Ca^{2+}-bound peptides ^{241}DAVLYSGATLDEAER^{255} and ^{256}LTEEELR^{262} emerged only when the receptor was incubated with Ca^{2+} before sample preparation for LC-MS/MS (*SI Appendix*, Figs. S7 and S8). Examination of other proteolytic PTHR fragments did not reveal additional Ca^{2+}-bound peptides (*SI Appendix*, Figs. S9–S11 and Table S1)

Given the well-known ability of acidic amino acid clusters to chelate Ca^{2+} and the presence of such clusters in each of the peptides identified by MS, we then generated two PTHR mutants wherein negatively charged aspartates (D) or glutamates (E) were substituted with Ser (S) side chains to impair Ca^{2+} chelation without significant impact on overall polarity: ^{251}DEAE^{254}→SSAS (noted ECL1-1), and ^{257}EEE^{259}→SSS (noted ECL1-2). The expression of receptor mutants was not affected (*SI Appendix*, Fig. S12). However, both ECL1 mutants were unable to engage in sustained cAMP production as efficiently as the wild-type (WT) receptor (Fig. 3*B*). Despite normal internalization, the PTH dissociated with markedly faster kinetics from receptor mutants compared with the WT receptor, consistent with more transient cAMP responses (Fig. 3*C*). Time courses of cAMP measurements for ECL1-1 and ECL1-2 receptor mutants in response to the PTH revealed markedly reduced sensitivity to Ca^{2+}, particularly, for ECL1-2 (Fig. 3*D*). Similarly, receptor mutants failed to mimic the effects of $[Ca^{2+}]$ on ligand binding that were observed for the WT receptor in saturation-binding experiments (Fig. 3 *E* and *F*). These

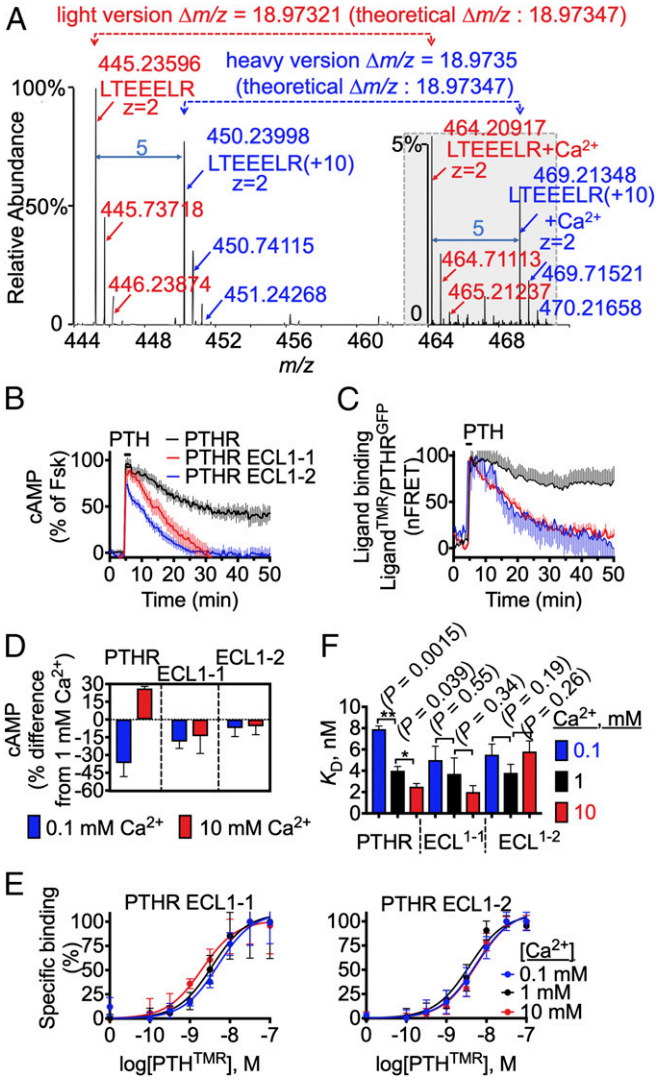

Fig. 3. Involvement of the receptor's ECL1 in Ca^{2+} allostery. (*A*) Representative MS of the tryptic digest of the PTHR from SILAC experiments showing the identified peptide ^{256}LTEEELR^{262} located within the ECL1 of the receptor. The free and Ca^{2+}-bound versions of the peptide were detected simultaneously. The red and blue colors represent light and heavy versions of the peptide. The theoretical mass-to-charge differences (Δ*m*/*z*) between free and Ca^{2+}-bound peptides are shown for both light and heavy versions. The Δ*m*/*z* values of the corresponding light and heavy peptides are 5. For clarity, the MS peaks for Ca^{2+}-bound peptides are enlarged and highlighted in a gray box. (*B*) Averaged time courses of cAMP production in response to the PTH in HEK293 cells expressing the PTHR or the PTHR-ECL1 mutants measured by FRET. Individual cells were continuously perfused with a buffer or with the ligand (10 nM) for the time indicated by the horizontal bar. (*C*) Averaged dissociation time courses of the PTH-TMR from the WT (black) or the mutant $PTHR^{GFP}$ (ECL1-1—red, ECL1-2—blue). FRET recordings from HEK293 cells are shown as a normalized ratio. (*D*) The effect of 0.1 and 10 mM Ca^{2+} on cAMP response mediated by the 10 nM PTH in HEK293 cells expressing either the WT PTHR, or the ECL1 mutant receptors. cAMP responses were quantified by measuring the area under the curve from 0 to 35 min and are represented as percentage differences from the 1 mM Ca^{2+} effect. (*E*) Saturation-binding isotherms of the PTH^{TMR} to ECL1 mutants of the PTHR stably expressed in HEK293 cells. The mean ± SEM of $n = 3$ carried out in triplicate. (*F*) The bars represent the mean of the K_d values ± SEM of binding experiments shown in Figs. 1*C* and 3*E*. *Significantly different when $P < 0.05$. Time courses represent the mean value ± SEM of $n > 3$ with $n = 14$–26 cells/experiment.

results suggest that acidic residues within ECL1 of the PTHR serve as key determinants for mediating Ca^{2+} allostery and endosomal signaling by the PTH.

Positive Ca^{2+} Allostery Is Lost for the Hypocalcemia-Causing PTH Mutant. Although negatively charged amino acids within ECL1 of the PTHR clearly play a role in mediating allosteric modulation by Ca^{2+}, the lack of sensitivity to [Ca^{2+}] observed in PTHrP-induced cAMP time courses suggests an additional ligand-dependent component. Previous work has shown that amino acids 15–34 of the PTH are essential for endosomal signaling as M-PTH(1–14), a modified N-terminal PTH(1–14) fragment causes only transient cAMP production from the cell surface (8). We discovered that Ca^{2+} allostery was completely abolished for M-PTH(1–14) (*SI Appendix*, Fig. S13*B*), indicating that PTH residues 15–34 constitute a Ca^{2+}-sensitive region.

We next examined the PTH^{R25C}, a recently identified homozygous PTH variant wherein Arg at position 25 has been substituted with cysteine. Patients harboring this mutation present with severe hypocalcemia despite normal or even excess levels of the circulating hormone, likely due to the reduced efficacy of the PTH^{R25C} in stimulating cAMP production (11), but the molecular basis for impaired signaling remains poorly understood. Given the apparent correlation between the PTHR sensitivity to [Ca^{2+}] and the ability to promote normal cAMP responses, we questioned whether position 25 of the PTH plays a role in mediating Ca^{2+} allostery and thus endosomal signaling. Indeed, saturation-binding analysis and cAMP time-course experiments in HEK cells revealed that the PTH^{R25C} completely lacks sensitivity to [Ca^{2+}] (Fig. 4 *A* and *B*). Moreover, the PTH^{R25C}-induced cAMP generation was markedly shorter in duration than that of the WT hormone (Fig. 4*B*) with similar results obtained in primary calvarial osteoblasts isolated from mice and human renal tubular epithelial cells expressing the native receptor (*SI Appendix*, Fig. S14). Preventing the PTHR internalization by expressing the DynK44A dominant negative mutant had a minimal effect on cAMP mediated by the PTH^{R25C}, but fully blocked sustained cAMP production induced by the PTH (Fig. 4*C*) suggested that the PTH^{R25C} signaling is mainly restricted to the cell surface. Surprisingly, the inability of the PTH^{R25C} to sustain cAMP was not due to defective internalization and trafficking of ligand-bound PTHR into endosomes as revealed by similar Pearson's correlation coefficients between TMR-labeled ligands and either PTHR detected with anti-HA-Alexa 488 conjugated antibody or Rab5 labeled with GFP (Rab5-GFP) (Fig. 4*D* and *SI Appendix*, Fig. S12*D* the WT lane and *SI Appendix*, Fig. S15).

To investigate the structural determinants of the PTH^{R25C} deficiency to mediate sustained cAMP responses, we employed circular dichroism (CD) to monitor secondary structure elements in the PTHR ligands. CD spectra for the PTH showed the two characteristic minima at 208 and 222 nm of α-helical peptides (*SI Appendix*, Fig. S16*D*), and the PTH^{R25C} exhibited similar spectral properties and retained the same α-helicity. Hence, the aberrant signaling of the PTH^{R25C} is unlikely caused by a conformational defect in the peptide. Given that the mutation-carrying C-terminal part of the PTH comprising residues 15–34 interacts with the receptor ectodomain (N-PTHR) (16), we next examined the PTH^{R25C} binding to the purified N-PTHR (*SI Appendix*, Fig. S16*E*). To this end, we performed isothermal titration calorimetry (ITC) measurements to determine the affinity and thermodynamic parameters of hormone binding (*SI Appendix*, Fig. S16 *A*–*C*). The ITC measurements revealed that the interaction of both ligands had similar affinity and was governed by the same mechanism: favorable enthalpy (ΔH ~ −20 kcal/mol) indicating that hydrogen bonds as well as polar and electrostatic attractions contribute

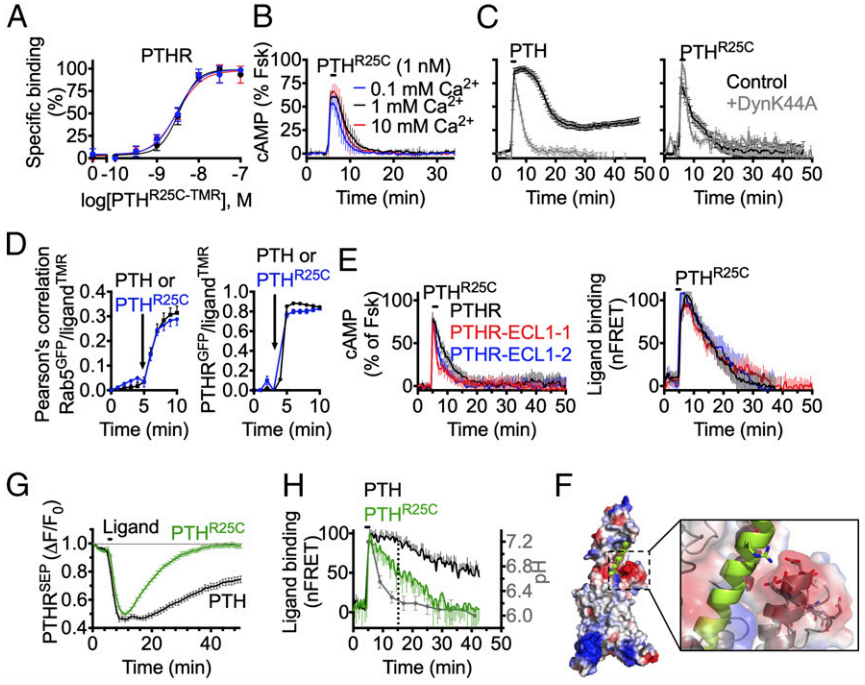

Fig. 4. Involvement of R25 of the PTH in interaction stabilization and receptor signaling. (*A*) Saturation-binding isotherms of the PTH-$R25C^{TMR}$ to the PTHR stably expressed in HEK293 cells with [Ca^{2+}] = 0.1 (blue), 1 (black), or 10 (red) mM. The mean ± SEM of $n = 3$ experiments carried out in triplicate. (*B*) Averaged time courses of cAMP production in response to the PTH^{R25C} in HEK293 cells expressing the PTHR in the presence of a range of [Ca^{2+}] measured by FRET. (*C*) Time courses of cAMP production in response to the PTH (*Right*) or the PTH^{R25C} (*Left*) in HEK293 cells expressing the PTHR. Experiments were run at two conditions: cells expressing only the PTHR (black), and cells coexpressing the PTHR and DynK44A dominant negative mutant (gray). Individual cells were perfused with a buffer or with the ligand (10 nM) for the time indicated by the horizontal bar. (*D*) Pearson's correlation values obtained from colocalization experiments between PTH-TMR or PTH^{R25C}-TMR with anti-HA-Alexa 488 (the $PTHR^{AF488}$, *Right*) or the early endosome marker Rab5-GFP (*Left*). The individual channel and merged images are shown in *SI Appendix*, Figs. S12*D* and S15. The arrows indicate the time of ligand perfusion. (*E*) Averaged time courses of cAMP production in response to the PTH^{R25C} in HEK293 cells expressing the PTHR or the PTHR-ECL1 mutants (*Left*), and dissociation time courses of the PTH^{R25C}-TMR from WT or the mutant $PTHR^{GFP}$ also expressed in HEK293 cells (*Right*) measured by FRET. Individual cells were continuously perfused with buffer or with the ligand (10 nM) for the time indicated by the horizontal bar. (*F*) Homology model of the PTHR generated from GPCR-I-TASSER (32) with the modeled PTH. The PTHR is shown as an electrostatic surface, and the PTH is represented as a green helix. The PTH R25 points toward an acidic face of the PTHR, which consists of ECL1-1 and ECL1-2 residues; the PTH R25 and residues of ECL1-1 and ECL1-2 are shown as sticks. (*G*) Time courses of internalization and recycling of the $PTHR^{SEP}$ in response to a ligand, measured by time-lapse confocal microscopy with images acquired every 60 s. The baseline was established, and cells were perfused with a 100 nM ligand for 20 s then washed out. (*H*) Averaged dissociation time courses of the PTH-TMR from the $PTHR^{GFP}$. FRET recordings from HEK293 cells are shown as normalized ratios. Cells were perfused with a 50 nM ligand for 30 s then washed out. The gray line is a recording of pH using the PTH-fluorescein isothiocyanate in HEK293 cells expressing the PTHR C-terminally tagged with CFP. Time courses represent the mean value ± SEM of $n = 3$ with $n = 8$–20 cells/experiment.

to binding, which combined with unfavorable entropy ($-T\Delta S \sim 10$ kcal/mol), gave an equilibrium dissociation constant K_d in the low μM range for the PTH or the PTH^{R25C} binding to N-PTHR (*SI Appendix*, Fig. S16 *B* and *C*). The measured favorable enthalpy is in good agreement with the observed stabilizing hydrogen and electrostatic bond network in the crystal structure of the PTH(15–34) fragment bound to N-PTHR (16). Altogether, our ITC measurements indicated an unaltered interaction between C-terminal PTH or PTH^{R25C} fragments with the receptor N-terminal domain, ruling out its role in deficient signaling by the PTH^{R25C}.

We considered the possibility that R25 of the PTH engages in ionic interactions with the negatively charged residues within ECL1 of the PTHR because the reduced Ca^{2+} allostery and endosomal signaling observed with the PTH^{R25C} were mimicked by ECL1 receptor mutants (Fig. 4*E*). The R25 interaction with acidic residues within ECL1 is, indeed, supported by our homology model of the PTHR built to investigate possible structural interactions between the PTH and the ECL1 of the receptor (Fig. 4*F*). In this model, R25 faces the acidic regions on ECL1 of the PTHR at a distance compatible with salt bridge formation. In agreement with this hypothesis, the signaling deficits of the PTH^{R25C} were recapitulated when Arg25 in the PTH was replaced by Ser or Ala (PTH^{R25S} or PTH^{R25A}) (*SI Appendix*, Fig. S13*A*). The lack of R25 interaction with ECL1 acidic residues resulted in rather faster receptor recycling (Fig. 4*G*) due to the faster dissociation rate of the PTH^{R25C} indicating increased pH sensitivity of this mutant hormone (Fig. 4*H*), which is likely an underlying reason for its endosomal signal deficiency. Collectively, these results provide strong evidence that ionic interactions between R25 of PTH and ECL1 residues of the PTHR are required for positive allosteric modulation by Ca^{2+} that likely stabilize hormone interaction with the receptor and thus are a prerequisite for endosomal signaling.

Possible Structural Mechanisms of Ca^{2+} Allostery. The data presented above suggest that Ca^{2+} binding within acidic clusters of the receptor's ECL1 enhances interaction with the PTH and ABL. In the case of the PTH, Ca^{2+} coordination appears to promote Arg25 of the PTH interaction with ECL1 acidic clusters. The concomitant Ca^{2+} coordination and Arg25 binding by ECL1 acidic residue clusters could occur if ECL1 Ca^{2+} coordination site adopts an EF-hand-like calcium-binding motif. In such a case, a calcium-binding site would be formed by one or two acidic residues from each of the two acidic clusters, which possibly exposes the rest of the acidic residues for Arg25 binding, overall promoting Arg25 interaction with the acidic cluster in the presence of Ca^{2+}. Another possible mechanism might be anticipated where Arg25 itself participates in Ca^{2+} coordination through water molecules similarly as does Lys in the second calcium-binding domain of the Na^+–Ca^{2+} exchanger (17). In the case of ABL where position 25 is occupied by negatively charged glutamic acid (Glu), in contrast to positive Arg in the PTH, the ECL1 might adopt a different conformation than in the PTH-bound receptor, and the Ca^{2+} coordination site might be formed by ECL1 acidic residue clusters together with Glu25 of ABL. Such a flexible nature of ECL1 is supported by a recent high-resolution structure of the PTHR where the electron density for this fragment of the receptor is not resolved, suggesting that it may assume multiple conformations (18). Interestingly, Ca^{2+} appeared to have no effect on cAMP responses mediated by the PTHrP (*SI Appendix*, Fig. S3*C*), which has histidine at position 25, a shorter residue that cannot participate in Ca^{2+} chelation. Given the high similarity of ABL and the PTHrP, but opposing sensitivity to Ca^{2+} modulation together with the lack of Ca^{2+} allostery for the R25C mutant of the PTH, our study suggests that position 25 in the PTHR peptide ligands is a determinant of the sensitivity to Ca^{2+} allostery, making it an important site for the rational peptide analog design strategies.

Discussion

Over the past decades it has been well established that Na^+ acts as a negative allosteric modulator of numerous family A GPCRs where it binds to a conserved site within the seven transmembrane helix bundle and stabilizes an inactive state of the receptors (reviewed in ref. 19). In contrast, the divalent cations, such as Mg^{2+}, Ca^{2+}, and Mn^{2+}, have been found to positively modulate family A GPCRs (20–25), and Ca^{2+} is a known allosteric regulator of several family C GPCRs (reviewed in ref. 26) whereas being an orthosteric agonist of the calcium-sensing receptor. Here, we reveal cellular and molecular mechanisms of positive allosteric actions of Ca^{2+} on a medically important family B GPCR, the PTHR.

Indeed, the PTH is the indispensable endocrine hormone regulating blood levels of calcium and phosphate ions. The PTH binds and activates its cognate receptor PTHR in bones where it induces bone resorption that, in turn, releases ionic calcium from the mineralized bone matrix. Consequently, the receptor encounters elevated extracellular Ca^{2+} concentrations that can reach up to 40 mM (11). Here, we studied the effects of extracellular Ca^{2+} on the PTHR ligand binding and signaling. Our findings identify the ability of extracellular Ca^{2+} to act as an allosteric modulator of the PTHR activation by promoting cAMP signaling when $[Ca^{2+}] > 1$ mM and attenuating signaling when $[Ca^{2+}] < 1$ mM. We demonstrated that the sensitivity of the PTHR signaling to Ca^{2+} allostery is dependent on two acidic residue clusters in the first extracellular loop of the receptor where possible Ca^{2+} coordination may promote interaction with ligands, thus, increasing their residence time on the receptor.

Our investigation of the cellular and molecular bases of hypocalcemia caused by a novel PTH variant where the Arg residue at position 25 is mutated to Cys (13) revealed that this mutant has an impaired capacity to prolong cAMP responses from endosomes. The mutant hormone's conformation, binding affinity to the extracellular domain of the PTHR, and trafficking properties were comparable to WT PTH. However, we showed that the loss of R25 in the PTH^{R25C} renders this mutant insensitive to Ca^{2+} allostery and short acting. Our findings allow us to infer that R25 in the PTH might be a key residue interacting with acidic clusters of the receptor's ECL1, and Ca^{2+} coordination at this site may further promote and stabilize this interaction. We propose that Ca^{2+} allostery is a determinant of biased PTH agonism as it relates to the duration of the PTHR signaling. Furthermore, the observed loss of sensitivity to Ca^{2+} in the disease-causing PTH variant unveils an unexpected role of Ca^{2+} in the etiology of hypocalcemia.

Since PTH-induced PTHR activation results in the elevation of serum Ca^{2+} concentration, it seems counterintuitive to investigate the role of Ca^{2+} as a feedforward regulator of the PTHR signaling. Because of that and the foremost association of Ca^{2+} to the Ca^{2+}-sensing receptor, its role as an allosteric modulator of the PTHR has not been widely explored. Here, we found that extracellular Ca^{2+} contributes significantly to endosomal cAMP production by increasing the stability of agonist–PTHR complexes; a process that the disease associated point mutation in the PTH fails to induce. This paper demonstrates a clear Ca^{2+} allostery on the PTHR activation, however, the actual Ca^{2+}-binding pocket in the receptor needs to be confirmed by further high-resolution structural studies. Overall, these findings compel us to reconsider a fundamental function of extracellular Ca^{2+} in the PTHR signaling. A possible contribution of Ca^{2+} allostery for the physiological function of the PTHR could take place during the well-recognized catabolic action of the PTH that induces the release of Ca^{2+} from bone through the stimulation of bone resorption. The increase in local $[Ca^{2+}]$ in the bone microenvironment could provide a positive feedback loop facilitating calcium homeostasis via the

PTH/PTHR system. Pertinent to this process is the correlation between the inability of the PTH^{R25C} to maintain a normal blood calcium level and the lack of the allosteric effect of Ca^{2+} when this ligand binds the PTHR.

Prolonged cAMP generation from the endosomes was originally discovered for the PTHR (3), but its physiological relevance remained unknown until recently. The first reliable link between the endosomal cAMP response and its physiological outcome was provided by the finding that a long-acting PTH analog LA-PTH, which triggers substantially longer endosomal cAMP responses than the PTH, is also able to induce enhanced and prolonged blood Ca^{2+} elevation in mice and in monkeys compared with the PTH (27, 28). This link is further strengthened by this study demonstrating that the hypocalcemia-causing mutation in the PTH displays defective endosomal PTHR signaling. The opposing actions of the PTH and the PTH^{R25C} as they relate to endosomal cAMP production in cells and calcemic responses in a human patient provide a better understanding of the disease relevance of endosomal PTHR signaling, which is likely the primary signaling component of the PTH-mediated regulation of calcium homeostasis in vertebrates.

Materials and Methods

cAMP was assessed using FRET-based assays. Cells were transiently transfected with the FRET-based biosensor Epac1-CFP/YFP (29) for measuring cAMP. Measurements were performed and analyzed as previously described (30). In brief, cells plated on poly-D-lysine coated glass coverslips were mounted in Attofluor cell chambers (Life Technologies), maintained in a 4-(2-hydroxyethyl)-1-piperazineethanesulfonic acid (Hepes) buffer containing 150 mM NaCl, 20 mM Hepes, 2.5 mM KCl, 0.1–10 mM $CaCl_2$, 0.1% bovine serum albumin, and pH 7.4 and transferred on the Nikon Ti-E equipped with an oil immersion 40× numerical aperture 1.30 Plan Apo objective and a moving stage (Nikon Corporation). CFP and YFP were excited using a mercury lamp. Fluorescence emissions were filtered using a 480 ± 20 nm (CFP) and 535 ± 15 nm (YFP) filter set and collected simultaneously with a LUCAS electron-multiplying charge-coupled device camera (Andor Technology) using a DualView 2 (Photometrics) with a beam splitter dichroic long pass of 505 nm. Fluorescence data were extracted from a single cell using Nikon Element Software (Nikon Corporation). The FRET ratio for single cells was calculated and corrected as previously described (31). Individual cells were perfused with a buffer or with the ligand for the time indicated by the horizontal bar.

Additional detailed *Materials and Methods* are included in the *SI Appendix*.

ACKNOWLEDGMENTS. We thank Dr. Eric Xu (Van Andel Institute) for providing the plasmid encoding the N-terminal domain of the PTHR and Dr. Andrew Hinck (University of Pittsburgh) for sharing his ITC instrument. J.-P.V. thanks Samuel Gellman, Shi Liu (Department of Chemistry, University of Wisconsin, Madison) for performing CD experiments, and Tom Gardella (Endocrine Unit, MGH) for providing TMR-labeled peptides. Research reported in this paper was supported by the National Institute of Diabetes and Digestive and Kidney Disease and the National Institute of General Medical Sciences of the US National Institutes of Health under Grant Awards R01-DK102495, R01-DK111427, and R01-DK116780 (to J.-P.V.) and T32-GM008424 (to A.D.W.); the Cotswold Foundation Fellowship Awards (to F.G.J.-A., and A.D.W.); start-up funds from the Department of Pharmacology and Chemical Biology, and the Vascular Medicine Institute of the University of Pittsburgh, and the Hemophilia Center of Western Pennsylvania, and the Institute for Transfusion Medicine (to K.X.); the Basic Science Research Program of the National Research Foundation of Korea Grant NRF-2013R1A1A1A05005629 and Korea Research-Driven Hospitals Grant fostered for Gachon University Gil Medical Center Grant FRD2014-04 (to S.L.).

1. Gardella TJ, Vilardaga JP (2015) International Union of Basic and Clinical Pharmacology. XCIII. The parathyroid hormone receptors–Family B G protein-coupled receptors. *Pharmacol Rev* 67:310–337.
2. Vilardaga JP, Jean-Alphonse FG, Gardella TJ (2014) Endosomal generation of cAMP in GPCR signaling. *Nat Chem Biol* 10:700–706.
3. Ferrandon S, et al. (2009) Sustained cyclic AMP production by parathyroid hormone receptor endocytosis. *Nat Chem Biol* 5:734–742.
4. Calebiro D, et al. (2009) Persistent cAMP-signals triggered by internalized G-protein-coupled receptors. *PLoS Biol* 7:e1000172.
5. Kotowski SJ, Hopf FW, Seif T, Bonci A, von Zastrow M (2011) Endocytosis promotes rapid dopaminergic signaling. *Neuron* 71:278–290.
6. Eichel K, von Zastrow M (2018) Subcellular organization of GPCR signaling. *Trends Pharmacol Sci* 39:200–208.
7. Feinstein TN, et al. (2011) Retromer terminates the generation of cAMP by internalized PTH receptors. *Nat Chem Biol* 7:278–284.
8. Wehbi VL, et al. (2013) Noncanonical GPCR signaling arising from a PTH receptor-arrestin-Gβγ complex. *Proc Natl Acad Sci USA* 110:1530–1535.
9. Gidon A, et al. (2014) Endosomal GPCR signaling turned off by negative feedback actions of PKA and v-ATPase. *Nat Chem Biol* 10:707–709.
10. Jean-Alphonse FG, et al. (2017) β_2-adrenergic receptor control of endosomal PTH receptor signaling via Gβγ. *Nat Chem Biol* 13:259–261.
11. Silver IA, Murrills RJ, Etherington DJ (1988) Microelectrode studies on the acid microenvironment beneath adherent macrophages and osteoclasts. *Exp Cell Res* 175:266–276.
12. Mitra N, et al. (2013) Calcium-dependent ligand binding and G-protein signaling of family B GPCR parathyroid hormone 1 receptor purified in nanodiscs. *ACS Chem Biol* 8:617–625.
13. Lee S, et al. (2015) A homozygous [Cys25]PTH(1-84) mutation that impairs PTH/PTHrP receptor activation defines a novel form of hypoparathyroidism. *J Bone Miner Res* 30: 1803–1813.
14. Feinstein TN, et al. (2013) Noncanonical control of vasopressin receptor type 2 signaling by retromer and arrestin. *J Biol Chem* 288:27849–27860.
15. Zindel D, et al. (2016) Identification of key phosphorylation sites in PTH1R that determine arrestin3 binding and fine-tune receptor signaling. *Biochem J* 473:4173–4192.
16. Pioszak AA, Xu HE (2008) Molecular recognition of parathyroid hormone by its G protein-coupled receptor. *Proc Natl Acad Sci USA* 105:5034–5039.
17. Besserer GM, et al. (2007) The second Ca2+-binding domain of the Na+ Ca2+ exchanger is essential for regulation: Crystal structures and mutational analysis. *Proc Natl Acad Sci USA* 104:18467–18472.
18. Ehrenmann J, et al. (2018) High-resolution crystal structure of parathyroid hormone 1 receptor in complex with a peptide agonist. *Nat Struct Mol Biol* 25:1086–1092.
19. Katritch V, et al. (2014) Allosteric sodium in class A GPCR signaling. *Trends Biochem Sci* 39:233–244.
20. Pasternak GW, Snowman AM, Snyder SH (1975) Selective enhancement of [3H]opiate agonist binding by divalent cations. *Mol Pharmacol* 11:735–744.
21. Johansson B, Parkinson FE, Fredholm BB (1992) Effects of mono- and divalent ions on the binding of the adenosine analogue CGS 21680 to adenosine A2 receptors in rat striatum. *Biochem Pharmacol* 44:2365–2370.
22. Rodriguez FD, Bardaji E, Traynor JR (1992) Differential effects of Mg2+ and other divalent cations on the binding of tritiated opioid ligands. *J Neurochem* 59:467–472.
23. Mazzoni MR, Martini C, Lucacchini A (1993) Regulation of agonist binding to A2A adenosine receptors: Effects of guanine nucleotides (GDP[S] and GTP[S]) and Mg2+ ion. *Biochim Biophys Acta* 1220:76–84.
24. Burgmer U, Schulz U, Tränkle C, Mohr K (1998) Interaction of Mg2+ with the allosteric site of muscarinic M2 receptors. *Naunyn Schmiedebergs Arch Pharmacol* 357:363–370.
25. Ye L, et al. (2018) Mechanistic insights into allosteric regulation of the A_{2A} adenosine G protein-coupled receptor by physiological cations. *Nat Commun* 9:1372.
26. Urwyler S (2011) Allosteric modulation of family C G-protein-coupled receptors: From molecular insights to therapeutic perspectives. *Pharmacol Rev* 63:59–126.
27. Hattersley G, Dean T, Corbin BA, Bahar H, Gardella TJ (2016) Binding selectivity of abaloparatide for PTH-type-1-receptor conformations and effects on downstream signaling. *Endocrinology* 157:141–149.
28. Shimizu M, et al. (2016) Pharmacodynamic actions of a long-acting PTH analog (LA-PTH) in thyroparathyroidectomized (TPTX) rats and normal monkeys. *J Bone Miner Res* 31:1405–1412.
29. Nikolaev VO, Bünemann M, Hein L, Hannawacker A, Lohse MJ (2004) Novel single chain cAMP sensors for receptor-induced signal propagation. *J Biol Chem* 279: 37215–37218.
30. Gidon A, Feinstein TN, Xiao K, Vilardaga JP (2016) Studying the regulation of endosomal cAMP production in GPCR signaling. *Methods Cell Biol* 132:109–126.
31. Vilardaga JP (2011) Studying ligand efficacy at G protein-coupled receptors using FRET. *Methods Mol Biol* 756:133–148.
32. Zhang J, Yang J, Jang R, Zhang Y (2015) GPCR-I-TASSER: A hybrid approach to G protein-coupled receptor structure modeling and the application to the human genome. *Structure* 23:1538–1549.